A $\mathcal{C}^0$ Interior Penalty Method for 4th order PDEs

Dani Fojo

Universitat Politècnica de
Catalunya
daniel.fojo@estudiant.upc.edu

David Codony

Universitat Politècnica de
Catalunya
david.codony@upc.edu

***Sonia Fernández-Méndez**

Universitat Politècnica de
Catalunya
sonia.fernandez@upc.edu

∗Corresponding author

Resum *(CAT)*

En aquest treball desenvolupem i estudiem el comportament d'un mètode per a la solució d'EDPs de 4^{rt} ordre amb aproximacions d'Elements Finits $\mathcal{C}^0$ estàndar. El mètode es basa en una forma feble que introdueix integrals entre elements per imposar continuïtat $\mathcal{C}^1$ en forma feble. El mètode es desenvolupa per les equacions que modelitzen una placa de Kirchoff, però es preveu que l'extensió a altres EDPs de 4^{rt} ordre sigui natural. La convergència i aplicabilitat del mètode s'estudia amb exemples numèrics.

Abstract *(ENG)*

A method to solve 4th-order PDEs using the Finite Element Method (FEM) with standard $\mathcal{C}^0$ elements is derived and studied. It is based on a special weak form accounting for the discontinuous derivatives of the approximation and imposing their normal continuity across element sides in weak form. The method is developed for the equations of the deformation of a Kirchoff plate, but its extension to other 4th-order PDEs is expected to be straightforward. The accuracy and convergence of the resulting numerical approximation is studied with numerical experiments.

Societat
Catalana de
Matemàtiques

Institut
d'Estudis
Catalans

1. Introduction

There are two main strategies for the numerical solution of 4$^{\text{th}}$ order PDEs. The first one consists on considering an approximation space with $\mathcal{C}^1$ continuity to discretize a weak form involving 2$^{\text{nd}}$ order derivatives. The main drawback of this approach is that the definition of $\mathcal{C}^1$-continuous approximations on non-cartesian meshes, such as the ones necessary to adapt to non-rectangular domains, is really cumbersome. Thus, these approximations are limited to the solution of problems in rectangular domains or in combination with a technique for embedded domains; see for instance [3].

An alternative is splitting the 4$^{\text{th}}$ order PDE in two 2$^{\text{nd}}$ order PDEs, allowing the use of $\mathcal{C}^0$ Finite Element (FE) approximations. However, the approximation spaces for the primal unknown and the additional unknown must fulfil some conditions for stability that, again, lead to approximation spaces with cumbersome definitions, and difficult extension to high-order approximations; see for instance [4].

A not so common approach is considering a modified weak form suitable for standard $\mathcal{C}^0$ FE approximations, imposing continuity of the derivative in weak form. This is the strategy considered in this work.

The developed formulation is based on the ideas of the Interior Penalty Method (IPM) [1], which considers discontinuous approximations and imposes $\mathcal{C}^0$ continuity in weak form, in the context of 2$^{\text{nd}}$ order PDEs. Here, the same ideas are applied for 4$^{\text{th}}$ order PDEs, but considering $\mathcal{C}^0$ approximations and imposing the continuity of the derivative in weak form. The resulting weak form involves second order derivatives, two different types of Dirichlet and Neumann boundary conditions and punctual forces on corners of the boundary. It coincides with the one proposed and analyzed in [2], but without some limitations for the boundary conditions. The derivation here is based on the use of the surface divergence theorem, instead of considering a limit from rounded corners to sharp corners, leading to a more natural understanding of the contribution of interior and boundary corners (vertices). In addition, a convergence study based on numerical experiments, assessing the real applicability of the method, is included here, and an strategy based on an eigenvalue problem is also proposed for the estimate of the value for the stabilization parameter to ensure coercivity.

Einstein notation (repeated indexes sum over) is assumed in the whole text.

2. A $\mathcal{C}^0$ Interior Penalty Method for Kirchoff plates

The equations modelling the behaviour of a plate with the Kirchoff model are

$$\frac{\partial^2 \sigma_{ij}(u)}{\partial x_i \partial x_j} = f \quad \text{on } \Omega \tag{1a}$$

$$u = g_1 \qquad \text{on } \Gamma_D^1 \tag{1b}$$

$$\frac{\partial u}{\partial \mathbf{n}} = g_2 \qquad \text{on } \Gamma_D^2 \tag{1c}$$

$$t(u) = t_n \qquad \text{on } \Gamma_N^1 \tag{1d}$$

$$r(u) = r_n \qquad \text{on } \Gamma_N^2 \tag{1e}$$
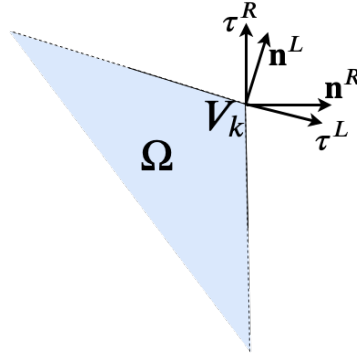
$$j_k(u) = j_k^{\text{ext}} \qquad \text{on } V_k \in V_N, \tag{1f}$$

Figure 1: Left and right tangent and normal vectors at a corner of the domain.

where

$$
\sigma_{ij}(u) = C_{ijkl}\frac{\partial^2 u}{\partial x_k \partial x_l}
$$

$$
t(u) = \left(\frac{\partial \sigma_{ij}(u)}{\partial x_i} - \nabla^\tau \cdot (\mathbf{n})n_i \sigma_{ij}(u)\right)n_j + \nabla^\tau \cdot (\boldsymbol{\sigma}(u) \cdot \mathbf{n}) \tag{2}
$$

$$
r(u) = \mathbf{n} \cdot \boldsymbol{\sigma}(u) \cdot \mathbf{n}
$$

$$
j_k(u) = \boldsymbol{\tau}_{\mathbf{k}}^{\mathbf{L}} \cdot \boldsymbol{\sigma}(u) \cdot \mathbf{n}_{\mathbf{k}}^{\mathbf{L}} + \boldsymbol{\tau}_{\mathbf{k}}^{\mathbf{R}} \cdot \boldsymbol{\sigma}(u) \cdot \mathbf{n}_{\mathbf{k}}^{\mathbf{R}},
$$

$\Gamma_D^1 \cup \Gamma_N^1 = \Gamma_D^2 \cup \Gamma_N^2 = \partial\Omega$, V_N are the vertices in the boundary in Γ_N^1, $\mathbf{n}$ is the exterior unitary normal vector, $\boldsymbol{\tau}$ is the tangent vector, and $\nabla^\tau \cdot \mathbf{f} := \tau_k \partial f_k / \partial \tau$. At each vertex, superscripts L and R refer to the left and right sides that meet there; see Fig. 1

In these equations u is the vertical displacement on the plate, the 4th order tensor $\mathbf{C}$ depends on the material, equation (1a) is the 4th-order PDE stating equilibrium with the vertical applied load f, equations (1b) and (1c) are the first and second Dirichlet conditions, equations (1d) and (1e) are the first and second Neumann conditions, and equation (1f) imposes punctual forces on the exterior vertices where the displacement is unknown. The boundary conditions (1c), (1e), and (1f), that may be not intuitive, can be justified from mechanical reasonings, or can be derived from the weak form of (1a).

Let us consider now a partition of Ω in subdomains Ω_e, that will in fact be the elements, and definitions for broken domain and boundaries, such as $\widehat{\Omega} = \bigcup_e \Omega_e$. Then, the problem can be stated as

$$
\frac{\partial^2 \sigma_{ij}(u)}{\partial x_i \partial x_j} = f \quad \text{on } \widehat{\Omega} \tag{3a}
$$

$$
u = g_1 \qquad \text{on } \widehat{\Gamma_D^1} \tag{3b}
$$

$$
\frac{\partial u}{\partial \mathbf{n}} = g_2 \qquad \text{on } \widehat{\Gamma_D^2} \tag{3c}
$$

$$
t(u) = t_n \quad \text{on } \widehat{\Gamma_N^1} \tag{3d}
$$

$$
r(u) = r_n \quad \text{on } \widehat{\Gamma_N^2} \tag{3e}
$$

$$
j_k(u) = j_k^{\text{ext}} \quad \text{on } V_k \in V_N \tag{3f}
$$

$$
[\![u\mathbf{n}]\!] = \mathbf{0} \quad \text{on } \Gamma \tag{3g}
$$

$$\left[\!\!\left[\frac{\partial u}{\partial \mathbf{n}}\right]\!\!\right] = 0 \qquad \text{on } \Gamma \tag{3h}$$

$$[\![t(u)]\!] = 0 \qquad \text{on } \Gamma \tag{3i}$$

$$[\![\mathbf{n}r(u)]\!] = \mathbf{0} \qquad \text{on } \Gamma \tag{3j}$$

$$\sum_{e \in E_k} j_k^e(u) = 0 \text{ on } V_k \in V_{int}, \tag{3k}$$

where Γ is the union of all interior sides Γ_f,

$$\Gamma = \left[\bigcup_e \partial\Omega_e\right] \setminus \partial\Omega = \bigcup_f \Gamma_f, \tag{4}$$

E_k is the set of elements touching the vertex V_k, V_{int} is the set of all interior vertices (i.e., vertices in Γ), and the jump operator is defined on each side Γ_f as $[\![a]\!] = a^L + a^R$, with a^L and a^R being the values from the elements Ω^L and Ω^R sharing the side. Note that the jump operator is always used including the normal vector, for instance, $[\![u\mathbf{n}]\!] = u^L\mathbf{n}^L + u^R\mathbf{n}^R = (u^L - u^R)\mathbf{n}^L$, thus, it is zero for a continuous function.

Equations (3g) and (3h) impose continuity of the displacement and its normal derivative. And equations (3i), (3j), and (3k) impose equilibrium of internal forces across sides between elements and on internal vertices.

Now, multiplying equation (3a) by an arbitrary function v, integrating over any element Ω_e and using twice integration by parts leads to

$$\int_{\Omega_e} vf \, d\Omega = \int_{\Omega_e} \frac{\partial^2 v}{\partial x_i \partial x_j}\sigma_{ij}(u) \, d\Omega - \int_{\partial\Omega_e} \frac{\partial v}{\partial x_i}\sigma_{ij}(u)n_j \, dS + \int_{\partial\Omega_e} v\frac{\partial \sigma_{ij}(u)}{\partial x_j}n_i \, dS \tag{5}$$

Now, the derivative in the first boundary integral can be split in normal and tangential derivative as $\frac{\partial v}{\partial x_i} = \tau_i\frac{\partial v}{\partial \boldsymbol{\tau}} + n_i\frac{\partial v}{\partial \mathbf{n}}$, and the integral for the tangential derivative can be expressed as

$$\int_{\partial\Omega_e} \tau_i\frac{\partial v}{\partial \boldsymbol{\tau}}\sigma_{ij}(u)n_j \, dS = \int_{\partial\Omega_e} \nabla^\tau \cdot (v\boldsymbol{\sigma}(u) \cdot \mathbf{n}) \, dS - \int_{\partial\Omega_e} v\nabla^\tau \cdot (\boldsymbol{\sigma}(u) \cdot \mathbf{n}) \, dS,$$

or, using the surface diverge theorem,

$$\int_{\partial\Omega_e} \tau_i\frac{\partial v}{\partial \boldsymbol{\tau}}\sigma_{ij}(u)n_j \, dS = \int_{\partial\Omega_e} \nabla^\tau\!\cdot\!(\mathbf{n})v\,\mathbf{n}\!\cdot\!\boldsymbol{\sigma}(u)\!\cdot\!\mathbf{n} \, dS + \sum_{s=1}^{\#sides\,\Omega_e} v\left[\boldsymbol{\tau}\cdot\boldsymbol{\sigma}(u)\cdot\mathbf{n}\right]_0^{end} - \int_{\partial\Omega_e} v\nabla^\tau\!\cdot\!(\boldsymbol{\sigma}(u)\cdot\mathbf{n}) \, dS,$$

where $[\cdot]_0^{end}$ denotes the value at the end minus the value at the beginning of the side, for each side of the element. Thus, equation (5) can now be written as

$$\begin{aligned}
\int_{\Omega_e} vf \, d\Omega = \;& \int_{\Omega_e} \frac{\partial^2 v}{\partial x_i \partial x_j}\sigma_{ij}(u) \, d\Omega \\
&+ \int_{\partial\Omega_e} v\left[\left(\frac{\partial \sigma_{ij}(u)}{\partial x_i} - \nabla^\tau\cdot(\mathbf{n})n_i\sigma_{ij}(u)\right)n_j + \nabla^\tau\cdot(\boldsymbol{\sigma}(u)\cdot\mathbf{n})\right] dS \\
&- \int_{\partial\Omega_e} \frac{\partial v}{\partial \mathbf{n}}[n_i\sigma_{ij}(u)n_j] \, dS - \sum_{k=1}^{\#vertices\,\partial\Omega_e} v\left(\tau_k^L\sigma(V_k)\mathbf{n}_k^L + \tau_k^R\sigma(V_k)\mathbf{n}_k^R\right),
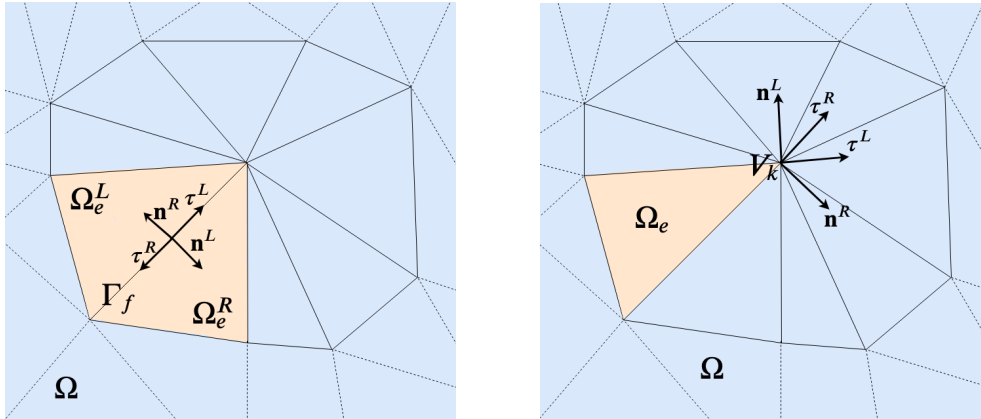\end{aligned} \tag{6}$$

Figure 2: Left and right tangent and normal vectors for a side Γ_f inside the mesh, and left and right tangent and normal vectors for an interior vertex of an arbitrary element Ω_e inside the mesh.

where the L and R indices refer to the values at the vertices from the left and right sides, and the tangent vectors $\tau_k^{L,R}$ point outward on the vertex for each side; see Fig. 2, right. Now, applying Definitions (2), equation (6) becomes

$$\int_{\Omega_e} vf \, d\Omega = \int_{\Omega_e} \frac{\partial^2 v}{\partial x_i \partial x_j} \sigma_{ij}(u) \, d\Omega + \int_{\partial\Omega_e} vt^e(u) \, dS - \int_{\partial\Omega_e} \frac{\partial v}{\partial \mathbf{n}} r^e(u) \, dS - \overset{\#vertices\,\partial\Omega_e}{\underset{k=1}{\sum}} vj_k^e(u), \quad (7)$$

where a superscript e remarks that the value is taken from element Ω_e. Summing (7) for all elements,

$$\int_{\widehat{\Omega}} vf \, d\Omega = \int_{\widehat{\Omega}} \frac{\partial^2 v}{\partial x_i \partial x_j} \sigma_{ij}(u) \, d\Omega + \int_{\partial\Omega} vt(u) \, dS - \int_{\partial\Omega} \frac{\partial v}{\partial \mathbf{n}} r(u) \, dS$$
$$+ \int_{\Gamma} v \left[\!\left[t(u) \right]\!\right] dS - \int_{\Gamma} \left[\frac{\partial v^L}{\partial \mathbf{n}^L} r^L(u) + \frac{\partial v^R}{\partial \mathbf{n}^R} r^R(u) \right] dS$$
$$- \sum_{V_k \in V_{int}} v \sum_{e \in E_k} j_k^e(u) - \sum_{V_k \in V_{ext}} v \sum_{e \in E_k} j_k^e(u),$$

where V_{int}, V_{ext} are the set of interior and exterior vertices, respectively. Now, using the identity

$$\frac{\partial v^L}{\partial \mathbf{n}^L} r^L(u) + \frac{\partial v^R}{\partial \mathbf{n}^R} r^R(u) = \left[\!\left[\frac{\partial v}{\partial \mathbf{n}} \right]\!\right] \{r(u)\} + \{\nabla v\} \cdot \left[\!\left[\mathbf{n} r(u) \right]\!\right],$$

with the mean operator $\{a\} := \frac{1}{2}\left(a^L + a^R\right)$, and the equilibrium equations (3i), (3j), and (3k), leads to

$$\int_{\widehat{\Omega}} vf \, d\Omega = \int_{\widehat{\Omega}} \frac{\partial^2 v}{\partial x_i \partial x_j} \sigma_{ij}(u) \, d\Omega + \int_{\partial\Omega} vt(u) \, dS - \int_{\partial\Omega} \frac{\partial v}{\partial \mathbf{n}} r(u) \, dS - \int_{\Gamma} \left[\!\left[\frac{\partial v}{\partial \mathbf{n}} \right]\!\right] \{r(u)\} \, dS - \sum_{V_k \in V_{ext}} v \sum_{e \in E_k} j_k^e(u).$$

Finally, replacing the Neumann boundary conditions, (1d), (1e), and (1f), imposing the first Dirichlet boundary condition in strong form (that is, (1b) and, consequently $v = 0$ on Γ_D^1), and adding some integrals with null sum (as a consequence of the $\mathcal{C}^1$ continuity of the solution (3h) and the second Dirichlet

boundary condition (1c)), we get the final weak form: find $u \in \mathcal{H}^2(\widehat{\Omega}) \cap \mathcal{C}^0(\Omega)$ such that $u = g_1$ on Γ_D^1 and $a(u, v) = \ell(v)$, for all $v \in \mathcal{H}^2(\widehat{\Omega}) \cap \mathcal{C}^0(\Omega)$ such that $v = 0$ on Γ_D^1, where

$$
\begin{aligned}
a(u, v) = {} & \int_{\widehat{\Omega}} \frac{\partial^2 v}{\partial x_i \partial x_j} \sigma_{ij}(u) \, d\Omega \\
& - \int_\Gamma \left[\!\!\left[\frac{\partial v}{\partial \mathbf{n}} \right]\!\!\right] \{r(u)\} \, dS - \int_\Gamma \{r(v)\} \left[\!\!\left[\frac{\partial u}{\partial \mathbf{n}} \right]\!\!\right] dS + \beta \int_\Gamma \left[\!\!\left[\frac{\partial v}{\partial \mathbf{n}} \right]\!\!\right] \left[\!\!\left[\frac{\partial u}{\partial \mathbf{n}} \right]\!\!\right] dS \\
& - \int_{\Gamma_D^2} \frac{\partial v}{\partial \mathbf{n}} r(u) \, dS - \int_{\Gamma_D^2} r(v) \frac{\partial u}{\partial \mathbf{n}} \, dS + \alpha \int_{\Gamma_D^2} \frac{\partial v}{\partial \mathbf{n}} \frac{\partial u}{\partial \mathbf{n}} \, dS,
\end{aligned}
\tag{8a}
$$

$$
\begin{aligned}
\ell(v) = {} & \int_{\widehat{\Omega}} vf \, d\Omega - \int_{\Gamma_N^1} vt_n \, dS + \int_{\Gamma_N^2} \frac{\partial v}{\partial \mathbf{n}} r_n \, dS + \sum_{V_k \in V_N} vj_k^{\text{ext}} \\
& - \int_{\Gamma_D^2} r(v)g_2 \, dS + \alpha \int_{\Gamma_D^2} \frac{\partial v}{\partial \mathbf{n}} g_2 \, dS.
\end{aligned}
\tag{8b}
$$

The terms added to the weak form recover symmetry and coercivity of the bilinear form, provided that parameters β and α are large enough. They also weakly enforce continuity of the normal derivative across elements interior sides (continuity along sides is given by the $\mathcal{C}^0$ continuity), and the second Dirichlet boundary condition. In fact, the parameters β and α act as penalty parameters, but differently to a non-consistent penalty formulation, moderate values of the parameters, of order $\mathcal{O}(h^{-1})$, provide convergence for any degree of approximation, avoiding the typical ill-conditioning problems of non-consistent penalty methods. Proper values for the parameters can be obtained solving an eigenvalue problem, as commented in Section 3.

The methodology considered here for the weak imposition of interface conditions and boundary conditions is inspired by the Interior Penalty Method [1], developed in the context of discontinuous approximations to weakly impose $\mathcal{C}^0$ continuity, and on Nitsche's method [6], developed for Dirichlet boundary conditions, here applied for the second Dirichlet boundary condition. Both methods are well known in the context of second-order PDEs. The difficulties for its application with fourth-order PDEs have been overcome here thanks to the use of the surface divergence theorem.

The FE solution can now be obtained replacing the classical $\mathcal{C}^0$ FE approximations in the weak form and solving the resulting linear system of equations for the nodal values.

3. Analysis of the β parameter

A study of the value of parameter β ensuring the coercivity of the bilinear form (8a), which can be easily replicated for parameter α, is presented next. It is inspired in the analysis developed in [3] for embedded domains. We consider the problem with $\Gamma_N^2 = \partial\Omega$ (i.e., without second Dirichlet boundary conditions), and a FE space V_0^h, which discretizes the space of functions in $\mathcal{H}^2(\widehat{\Omega}) \cap \mathcal{C}^0(\Omega)$ with null value on Γ_D^1. The matrix resulting from the discretization will be positive definite if $a(v, v) > 0$ for all non-null $v \in V_0^h$.

Using Cauchy–Schwartz inequality, the bilinear form can be bounded as

$$a(v, v) = \int_{\widehat{\Omega}} \frac{\partial^2 v}{\partial x_i \partial x_j} \sigma_{ij}(v) \, d\Omega - 2 \int_{\Gamma} \left[\!\!\left[\frac{\partial v}{\partial \mathbf{n}} \right]\!\!\right] \{r(v)\} \, dS + \beta \int_{\Gamma} \left[\!\!\left[\frac{\partial v}{\partial \mathbf{n}} \right]\!\!\right]^2 dS$$

$$\geq \int_{\widehat{\Omega}} \frac{\partial^2 v}{\partial x_i \partial x_j} \sigma_{ij}(v) \, d\Omega - 2 \left\| \left[\!\!\left[\frac{\partial v}{\partial \mathbf{n}} \right]\!\!\right] \right\|_{L^2(\Gamma)} \| \{r(v)\} \|_{L^2(\Gamma)} + \beta \left\| \left[\!\!\left[\frac{\partial v}{\partial \mathbf{n}} \right]\!\!\right] \right\|_{L^2(\Gamma)}^2.$$

Now, let us consider a constant c (depending only on the considered FE discretization space) such that

$$\| \{r(v)\} \|_{L^2(\Gamma)}^2 \leq c^2 \int_{\widehat{\Omega}} \frac{\partial^2 v}{\partial x_i \partial x_j} \sigma_{ij}(v) \, d\Omega \quad \forall v \in V_0^h. \tag{9}$$

Then, using Young's inequality $\left(ab \leq \frac{a^2}{2\varepsilon} + \frac{\varepsilon}{2} b^2 \, \forall a, b, \varepsilon > 0 \right)$, we have

$$a(v, v) \geq \left[1 - \frac{c^2}{\varepsilon} \right] \int_{\widehat{\Omega}} \frac{\partial^2 v}{\partial x_i \partial x_j} \sigma_{ij}(v) \, d\Omega + [\beta - \varepsilon] \left\| \left[\!\!\left[\frac{\partial v}{\partial \mathbf{n}} \right]\!\!\right] \right\|_{L^2(\Gamma)}^2 \tag{10}$$

for any $\varepsilon > 0$. Thus, the matrix will be positive definite if $\beta > c^2$.

In practice, β can be taken slightly larger than the largest eigenvalue of the generalized eigenvalue problem $\mathbf{KV} = \lambda \mathbf{MV}$, being $\mathbf{M}$ and $\mathbf{K}$ the matrices corresponding to the discretization of $\int_{\widehat{\Omega}} \frac{\partial^2 v}{\partial x_i \partial x_j} \sigma_{ij}(u) \, d\Omega$ and $\int_{\Gamma} \{r(v)\} \{r(u)\} \, dS$, respectively. Moreover, under nested mesh refinement, with characteristic element size h, the matrices $\mathbf{M}$ and $\mathbf{K}$ scale as h^{-3} and h^{-2}, respectively, thus, the maximum eigenvalue (and parameter β) scales as h^{-1}.

4. Numerical Experiments

4.1 Convergence and sensitivity to β parameter

As commented in the introduction, [2] presents a theoretical convergence analysis of the formulation valid for smooth boundaries (without corners) or pure Dirichlet boundary conditions. The conclusion of the analysis is that the method is convergent for large enough parameter β, but too large values may lead to suboptimal convergence. To assess the applicability of the method in real computations, the accuracy and convergence of the numerical solution of (1a), with boundary conditions (1b) and (1e) in the whole boundary, is tested next with

$$\sigma_{ij}(u) = \frac{\tau^3}{12} \left(2\mu \frac{\partial^2 u}{\partial x_i \partial x_j} + \lambda \frac{\partial^2 u}{\partial x_k \partial x_k} \delta_{ij} \right),$$

and material parameters $\tau = \lambda = \mu = 1$, in a square domain $\Omega = [0, 1]^2$. The body force f, the Dirichlet boundary value g_1 and the second Neumann boundary value r_n are chosen in accordance with the analytical solution $u(x, y) = x^4 y$. Note that with this boundary conditions, the method depends only on β, and not on the parameter associated to second Dirichlet boundary conditions α.

Fig. 3 shows the evolution of the L^2 error of the displacement under uniform refinement with characteristic element size h. Optimal convergence would lead to errors $\|u - u^h\|_{L_2} = \mathcal{O}(h^{p+1})$ for degree of
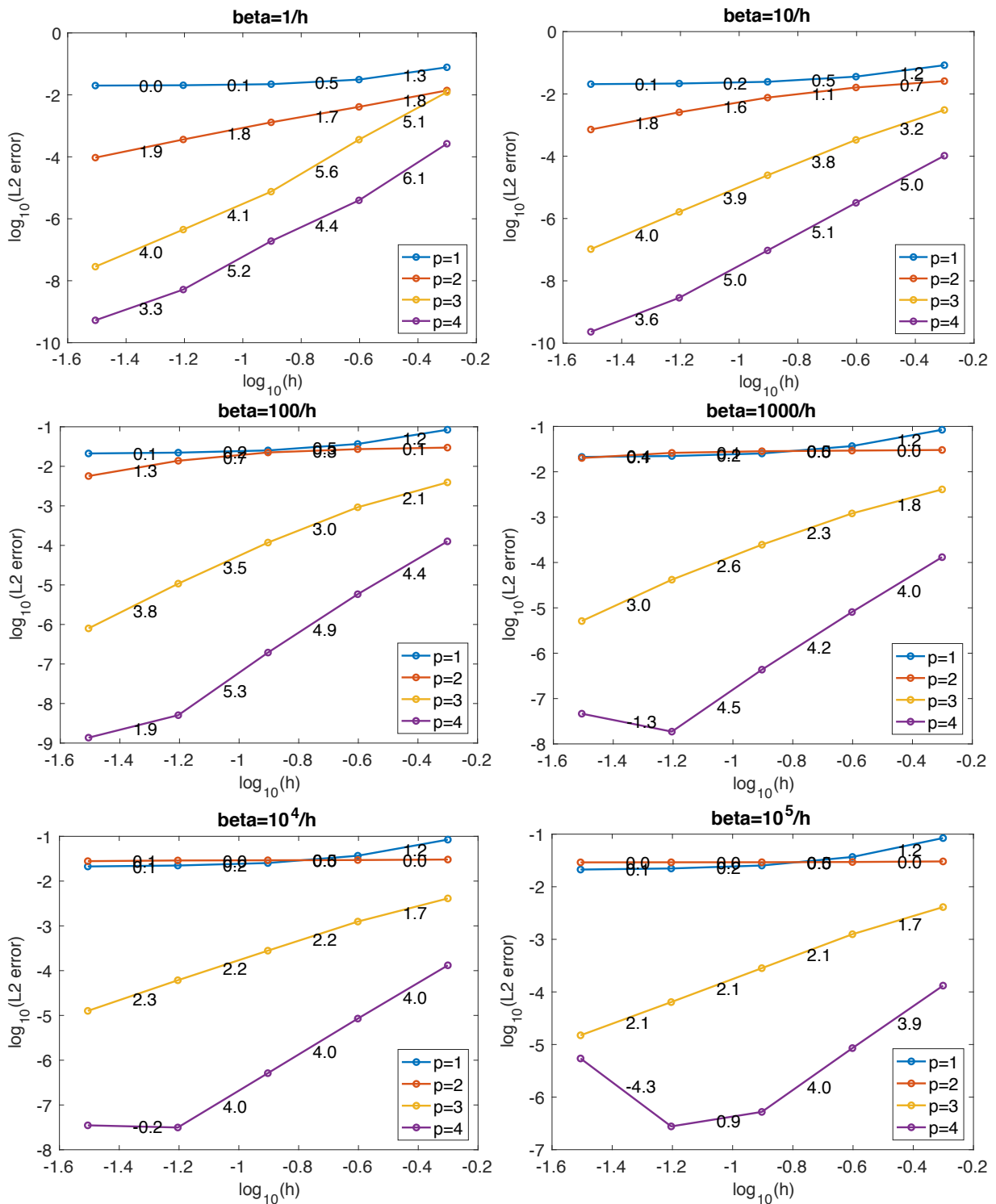
Figure 3: Convergence plots for different values of β and different degrees p. The numbers indicate the slopes of the segments.

approximation p, which would correspond to slope $p + 1$ in the plots. As expected, for degree $p = 1, 2$, the approximation space is not rich enough to weakly impose continuity of the derivatives and at the same time properly approximate the solution. This kind of locking leads to poor accuracy and convergence. However, for degree $p \geq 3$, a reasonably large range for β $((1 - 100)\tau^3/h$ for $p = 3)$ provides optimal convergence. Higher values of β lead to slightly suboptimal convergence, but still provide accurate results and good convergence. Much higher values of β are not recommended mainly because they may lead to a very ill-conditioned matrix, but also because we expect a continuous degradation in the convergence and accuracy due to the locking associated to a too strong imposition of the continuity of the derivative.

Thus, in practice, the recommendation is using a value of β slightly larger than the one corresponding to the maximum eigenvalue of the problem in Section 3. It is also worth noting that, assuming material parameters λ and μ constant or in a small range, $\mathbf{M}$ scales as $\tau^3 h^{-2}$, $\mathbf{K}$ scales as $\tau^6 h^{-3}$, and, therefore, the maximum eigenvalue scales as τ^3/h. Consequently, if the eigenvalue problem is solved for a particular mesh and a particular value of τ, the value for β for finer nested meshes, or other values of τ, can be estimated without solving the eigenvalue problem.
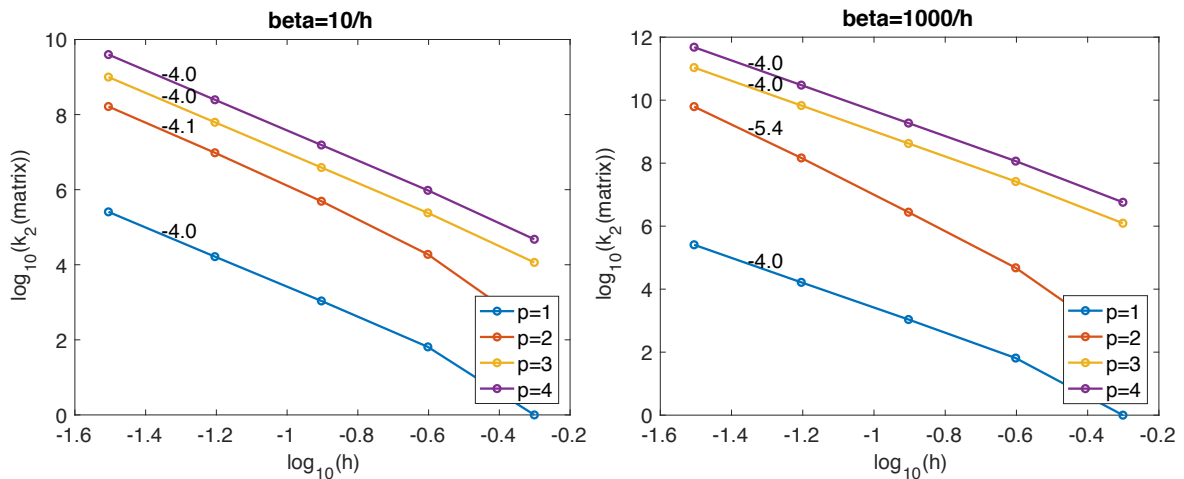

Figure 4: Condition number for degrees $p = 1, \dots, 4$, and for two different values of β, varying the element size h.

Fig. 4 shows the condition number of the matrix corresponding to the discretization of the problem for two different values of β, both above the bound for positiveness of the matrix. As expected, the condition number increases when increasing β. In addition, we observe an increase in the condition number as $\mathcal{O}(h^{-4})$, that is the expected behaviour for the numerical solution of a fourth-order PDE, regardless of the discretization method.

4.2 Plate under uniform distributed load

A more realistic problem is solved in this section to demonstrate the applicability of the proposed method: a plate under a uniformly distributed applied load of $f = 100$Pa. In this case, the material parameters are $\mu = E/(2(1 + \nu))$ and $\lambda = \nu E/(1 - \nu^2)$, with Young's modulus $E = 200 \cdot 10^9$Pa, Poisson's ratio $\nu = 0.28$ and thickness of the plate $\tau = 0.001$m, corresponding to a thick steel plate taken from [5]. The problem is solved on the $p = 4$ mesh depicted in Fig. 5, discretizing a plate of 1×1 meters. The considered penalty
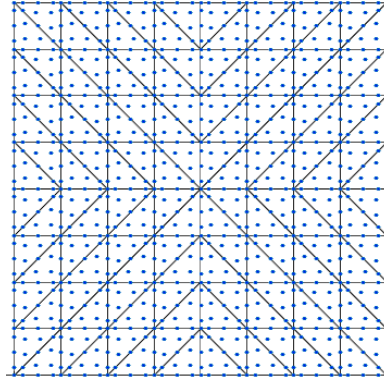
Figure 5: FE mesh. Blue dots are nodes for the $p = 4$ approximation.

parameters are $\beta = \alpha = 10\tau^3\mu/h = 781.25/h$ with element size $h = 0.125$m. Fig. 6 shows the solution for a simply supported plate (left) and a clamped plate (right). As expected, deformations are much larger for the simply supported plate.
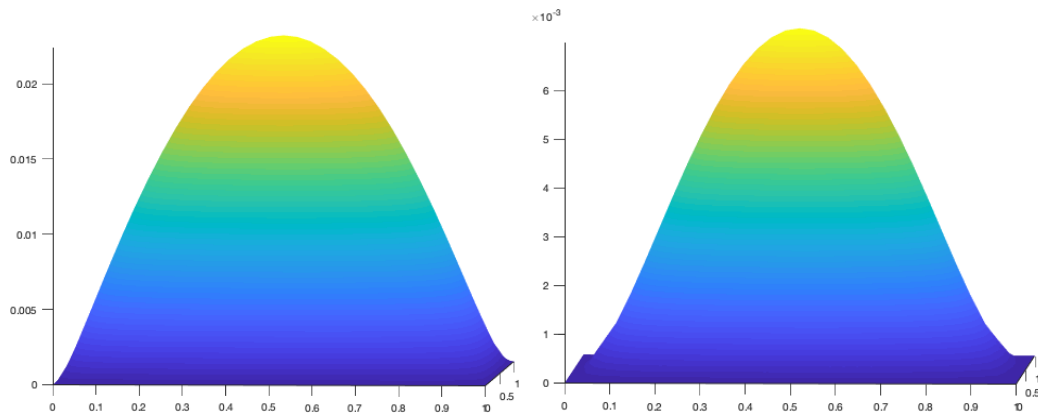

Figure 6: Solution of the problem with distributed load for a simply supported plate (left) and a clamped plate (right).

In both cases the first boundary condition is $u = 0$ on $\partial\Omega$. The second boundary condition is $r_n(u) = 0$ (Neumann) for the simply supported plate, and $\partial u/\partial n$ (Dirichlet) for the clamped plate. The null normal derivative on the boundary can be clearly observed in the right solution, corresponding to the clamped plate.

5. Conclusions and final remarks

A method for the solution of 4th-order PDEs, with standard $\mathcal{C}^0$ FE approximations, has been proposed. The method has been developed and tested for the solution of the equations of Kirchoff plates. It is based on a formulation that weakly imposes $\mathcal{C}^1$ continuity across element sides. Numerical experiments are in agreement with the theoretical analysis in [2]: a large enough penalty parameter β is needed to ensure

coercivity of the bilinear form, and convergence, but, on the other hand, too large β parameters may lead to suboptimal convergence. However, the numerical experiments show that a wide range of β parameter, within 3 orders of magnitude of difference, provides optimal convergence for degree $p \geq 3$, demonstrating the robustness of the method in practice. In fact, even for very large parameters, that should in practice not be considered to avoid ill-conditioning, the loss of optimal convergence is not catastrophic, since accurate results are still obtained.

The method is promising for the solution of other problems modelled by 4th-order PDEs, such as the ones modelling strain-gradient elasticity or flexoelectricity, overcoming the inconveniences or limitations of other techniques. Differently to *B*-spline approximations or Hermite interpolants, the discretization with standard FE allows the use of non-cartesian meshes, fitting to the boundary of non-rectangular domains, without the need to use a technique for embedded domains in non-fitted meshes, and avoiding the typical ill-conditioning problems related to the so-called cut elements. On the other hand, standard $\mathcal{C}^0$ FEs are easy to define and implement for any degree, differently to mixed approximations whose definition is cumbersome and not developed for high-order approximations and, in addition, involve additional unknowns increasing the computational cost.

In the next future, we aim to apply the same methodology to other 4th-order PDEs, and study its applicability and robustness in real applications of interest.

References

[1] D.N. Arnold, "An interior penalty finite element method with discontinuous elements", *SIAM J. Numer Anal* **4** (1982), 742–760.

[2] S.C. Brenner and L.Y Sung, "$\mathcal{C}^0$ Interior penalty methods for fourth order elliptic boundary value problems on polygonal domains", *Journal of Scientific Computing* **22–23** (2005), 83–118.

[3] D. Codony, O. Marco, S. Fernández-Méndez, and I. Arias, "An immersed boundary hierarchical *B*-spline method for flexoelectricity", *Computer Methods in Applied Mechanics and Engineering* **354** (2019), 750–782.

[4] F. Deng, Q. Deng, W. Yu, and S. Shen, "Mixed finite elements for flexoelectric solids", *Journal of Applied Mechanics* **84**(8) (2017).

[5] D.B. Miracle, S.L. Donaldson, D. Scott, et al., *ASM handbook* (2001) 21.

[6] J. Nitsche, "Über ein variationsprinzip zur lösung von Dirichlet-problemen bei verwendung von teilräumen, die keinen randbedingungen unterworfen sind", *Abhandlungen aus dem mathematischen Seminar der Universität Hamburg* **36** (1971), 9–15.